FEM Simulation of Orthogonal Machining of Al 6101-T6 and Inconel 718 Using Johnson-Cook Constitutive Model

Gabriel de Paiva Silva[1], Leonel Leonardo Delgado Morales[2], Déborah de Oliveira[1], Lucival Malcher[1]

[1]*Dept. of Mechanical Engineering, Faculty of Technology, University of Brasília*
Campus Darcy Ribeiro, Asa Norte, Zip-Code 70.910-900, Distrito Federal, Brazil
dpaivagabriel@gmail.com
[2]*Institute of Design and Industrial Methods, Faculty of Engineering Sciences, Austral University of Chile*
Miraflores Campus, General Lagos 2086, Valdivia, Chile
leonel.delgado@uach.cl

Abstract. Traditional machining processes such as milling and turning consist in using a cutting tool with defined geometry to give shape to a workpiece by removing material in the form of chips. The Finite Element Method (FEM) can be used to simulate the metal cutting procedure and predict output variables such as chip morphology and cutting forces, facilitating the optimization of machining parameters and reducing experimental costs. Thus, the present work aims to simulate machining operations to conduct a numerical analysis of chip morphology and cutting forces in different materials. The nickel superalloy Inconel 718, which is considered a hard-to-cut material, was chosen for a comparative study with the aluminum alloy Al 6101-T6, considered a material of good machinability. The mechanical properties of both materials were characterized using the Johnson-Cook constitutive model in the simulations, whereas the cutting tool was modelled as a rigid body. The results show that machining of Inconel 718 leads to worse chip formation, higher residual stresses, and higher cutting forces than Al 6101-T6, which is expected from literature.

Keywords: Finite Element Method, Inconel 718, Al 6101-T6, Chip Formation.

1 Introduction

Traditional machining processes involve the removal of material from a workpiece in the form of chips by using a cutting tool. In general, machining operations have the objective of efficiently manufacturing mechanical components or features with dimensional and geometrical precision, minimizing material waste and tool wear. The ideal cutting conditions of a machining operation depend on several aspects, including the mechanical properties of the materials of the workpiece and the tool, as well as cutting parameters such as depth of cut, feed rate, cutting speed, cutting forces, and many others. In order to reduce experimental costs, machining operations can be simulated numerically using an orthogonal cut modelling and the finite element method (FEM). In FEM machining simulations, different responses can be observed depending on the properties of the machined material, the geometry of the instances and machining parameters [1]. Besides, simulations of machining permit the analysis of variables that are difficult to obtain experimentally [2].

The machinability of a metallic alloy characterizes how easily the material can be sheared by a cutting tool. A simple change in the geometry of the tool or the presence of alloying elements in the machined material can drastically change machinability, therefore this parameter is highly variable [3]. Aluminum alloys, in general, tend to have good machinability due to their low hardness and density, although problems related to chip adhesion can be encountered if excessive heat is not controlled during machining [4]. Nickel-based superalloys, on the other hand, are known as hard-to-cut materials for several factors, including their high hardness and strength under elevated temperatures, high degree of work hardening, poor thermal conductivity, and high tendency of formation of built-up edge [5].

Therefore, the objective of this work is to promote a comparative study of machinability of two different alloys based on FEM numerical simulations. The materials chosen are: the aluminum alloy Al 6101-T6, which is a versatile material used in a wide range of applications [6]; and Inconel 718, a nickel superalloy usually used for

applications in harsh environments due to its excellent mechanical strength, creep resistance and corrosion resistance [7]. Machining of Inconel 718, as opposed to Al 6101-T6, presents many challenges associated with high cutting forces, bad surface quality, rapid tool wear rates and short lifespan of the cutting tool. Through the numerical simulations, the orthogonal cut of the two materials was performed in identical machining conditions, in order to analyze the effect of the material properties in the morphology of the chip, the stress distribution and the cutting forces.

2 Methodology

2.1 Johnson-Cook constitutive model

In the FEM simulations of machining, the mechanical properties of the materials were characterized using Johnson-Cook (JC) constitutive model [8]. According to JC model, the hardening rule of a material depends on the accumulated plastic strain, the accumulated plastic strain rate, and the temperature, according to eq. (1):

$$\sigma_y(\bar{\varepsilon}^p, \dot{\bar{\varepsilon}}^p, T) = [\mathrm{A} + \mathrm{B}(\bar{\varepsilon}^p)^n][1 + \mathrm{C}\ln(\dot{\bar{\varepsilon}}^{p*})](1 - T^{*m}). \quad (1)$$

In eq. 1, σ_y represents the hardening rule of the material, $\bar{\varepsilon}^p$is the accumulated plastic strain, $\dot{\bar{\varepsilon}}^p$ is the accumulated plastic strain rate and T is the temperature. The terms A, B and n are material constants that represent the initial yield stress, the isotropic hardening modulus, and the exponent of hardening, respectively. The parameters C and m control the effects of $\dot{\bar{\varepsilon}}^p$ and T. The terms $\dot{\bar{\varepsilon}}^{p*}$ and T^* are the dimensionless plastic strain rate and the homologous temperature, respectively, and are calculated according to eq. (2) and eq. (3):

$$\dot{\bar{\varepsilon}}^{p*} = \frac{\dot{\bar{\varepsilon}}^p}{\dot{\bar{\varepsilon}}_0^p}; \quad (2)$$

$$T^* = \frac{T - T_r}{T_m - T_r}. \quad (3)$$

In eq. (2) and eq. (3), $\dot{\bar{\varepsilon}}_0{}^p$represents the reference accumulated plastic strain rate, T is the current temperature, T_r is the room temperature and T_m is the melting temperature.

The failure model based on Johnson-Cook considers fracture of individual elements, assuming that damage is accumulated linearly according to eq. (4), where I_{JC} is the JC fracture indicator and ε_f is the equivalent plastic strain at fracture:

$$I_{JC} = \int_0^{\varepsilon_f} \frac{\dot{\bar{\varepsilon}}^p}{\varepsilon_f}. \quad (4)$$

According to JC, the equivalent plastic strain at fracture is a function of the stress triaxiality η, which is the ratio between hydrostatic pressure and the von Mises equivalent stress, as well as the dimensionless plastic strain rate $\dot{\bar{\varepsilon}}^{p*}$ and homologous temperature T^*, according to eq. (5):

$$\varepsilon_f = [D_1 + D_2 \exp(D_3\,\eta)][1 + D_4 \ln(\dot{\bar{\varepsilon}}^{p*})][1 + D_5 T^*], \quad (5)$$

where D_1, D_2, D_3, D_4 and D_5 are material parameters that need to be calibrated by adjusting experimental and numerical data.

The JC parameters of Inconel 718 and Al 6101-T6 used in this work were obtained by Erice and Gálvez [9] and Malcher et al. [10]. The numerical values are shown in Tab. 1.

Table 1. Johnson-Cook damage and plasticity parameters of the workpiece materials.

Parameter	Value for Inconel 718	Value for Al 6101-T6
D_1	0.04	0.071
D_2	0.75	1.246

D_3	-1.45	-1.142
D_4	0.04	0.147
D_5	0.89	0.1
Melting temperature	1,800 °C	600 °C
Transition temperature	25 °C	20 °C
A	1,200 MPa	1,480 MPa
B	1,284 MPa	3,410 MPa
C	0.006	0.001
m	1.20	0.859
n	0.54	0.183
Reference strain rate	0.001 s^{-1}	1 s^{-1}
Young modulus	185,000 MPa	70,000 MPa
Density	8.19×10^{-6} kg/mm^3	2.7×10^{-6} kg/mm^3
Poisson coefficient	0.33	0.27

2.2 Modelling of orthogonal cutting

The simulations were performed using standard database explicit models on Abaqus CAE, which is a commercial software for FEM analysis. Firstly, the cutting tool and the workpiece were modeled using 2D sketches with the dimensions in millimeters shown in Fig. 1. Then, to create 3D instances, the 2D sketches were extruded in the Z direction. The extrusion lengths are 10 millimeters for the tool and 8 millimeters for the workpiece.

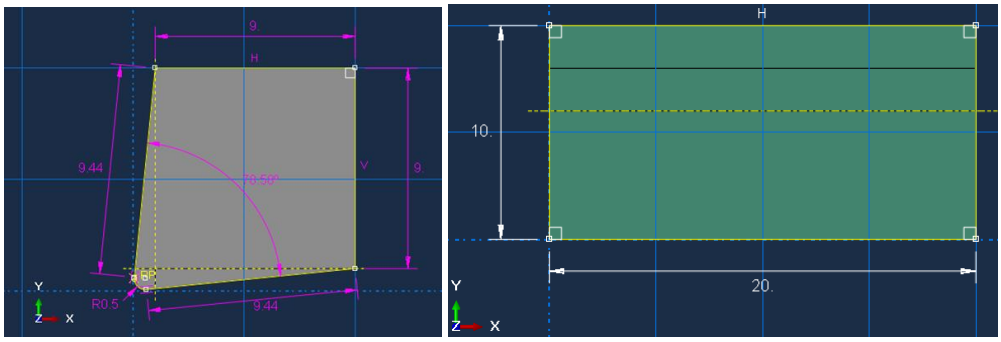

Figure 1. Sketches of the tool (left) and workpiece (right).

The cutting tool was modelled as a rigid body, whereas the properties of Inconel 718 and Al 6101-T6 were set for the workpiece in the respective simulations. In both simulations, the inferior edge of the workpiece was fixed, and a displacement was applied to the tool so as to simulate the orthogonal cut process. The instances were assembled, and interaction was established with friction coefficient 0.2. The instances were discretized with 3D elements, with finer discretization in the region of contact between the tool and the workpiece, as shown in Fig. 2. The simulation of failure of the workpiece material on Abaqus occurs by element deletion, so when each individual finite element suffers deformation beyond a specified limit, the element is deleted, so as to simulate shearing and chip formation.

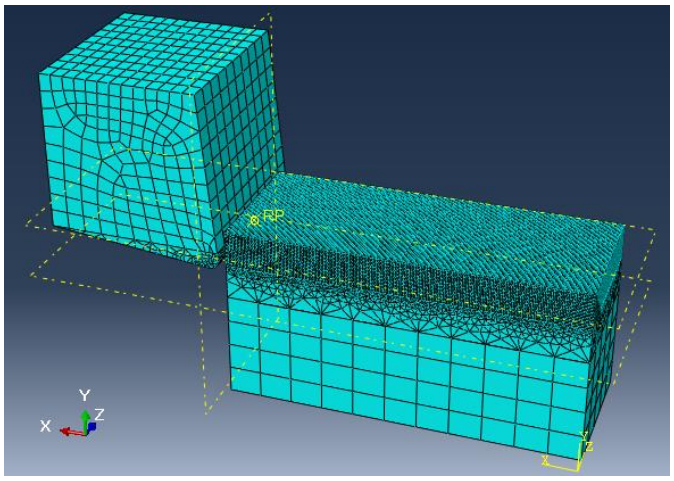

Figure 2. Assembly of the cutting tool and the workpiece discretized into finite elements.

Each simulation was carried out at a frequency of 20 evenly spaced time intervals, and the von Mises stress distribution and the cutting forces were monitored throughout the process. The cutting speed of the tool was set at 10 m/min and the depth of cut, which is the vertical distance between the top edge of the workpiece and the lowest point of the tool, was set at 1.25 mm.

3 Results and discussion

3.1 Chip formation

The morphology of the chips at different machined lengths for Al 6102-T6 and Inconel 718 are shown in Fig. 3 and Fig. 4, respectively. The color gradient represents the von Mises stress distribution in Pa.

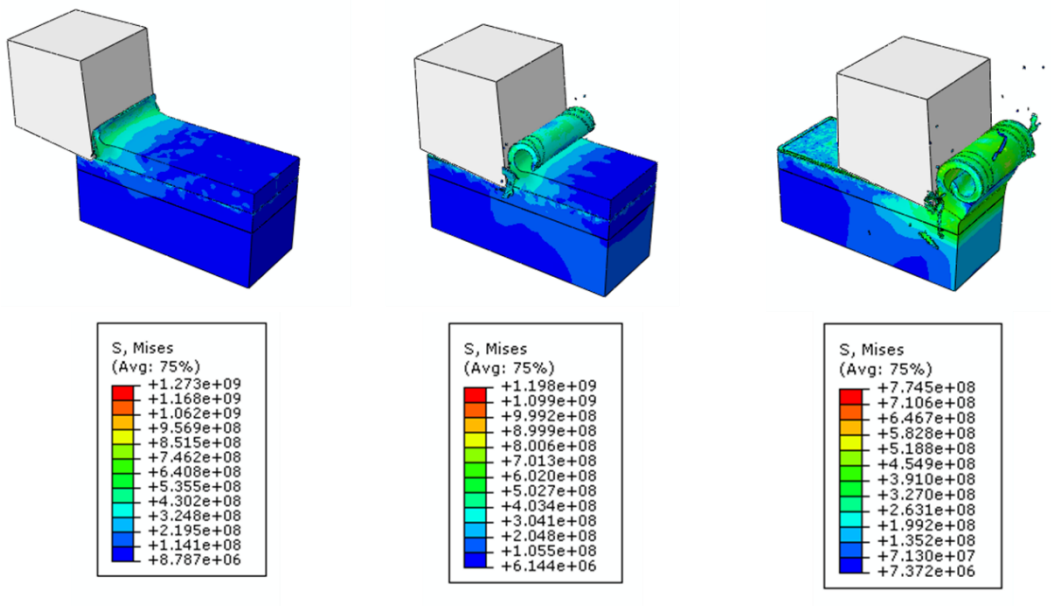

Figure 3. Chip morphology and von Mises stress distribution for Al 6101-T6.

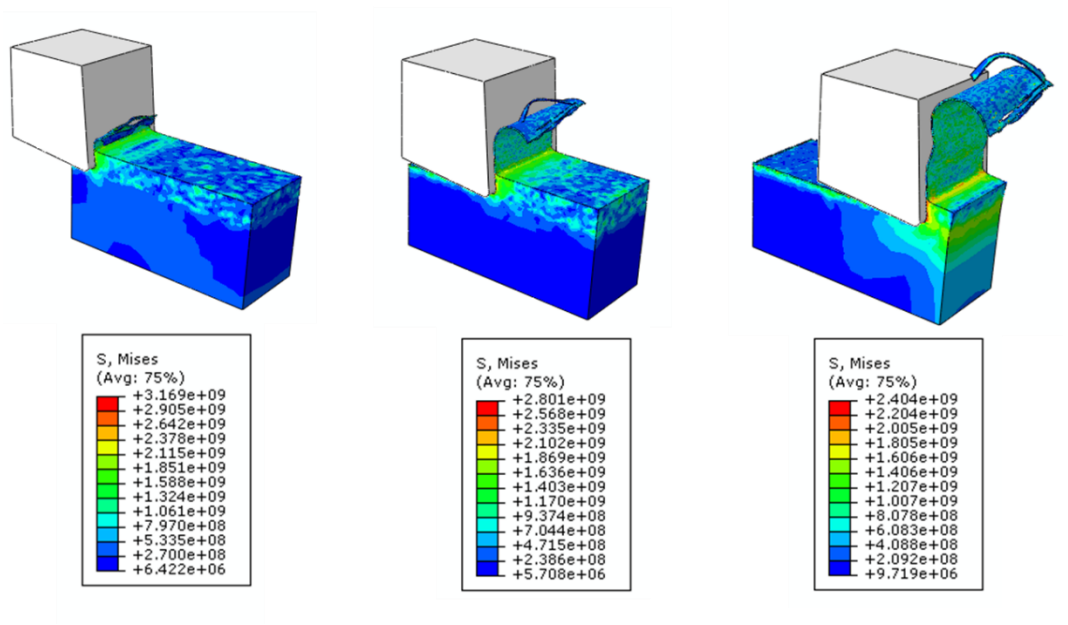

Figure 4. Chip morphology and von Mises stress distribution for Inconel 718.

By comparing the results of Fig. 3 and Fig. 4, it is possible to observe that the Al 6101-T6 chip is thicker than the Inconel 718 chip. This is probably due to the failure criterion established to the finite elements and the stresses to which the elements are subjected in the region of interface between the workpiece and the tool. Inconel 718 is more resistant; therefore, a great number of elements tend to either remain attached to the workpiece with high residual stresses or to be deleted because of excessive deformation. The aluminum alloy, on the other hand, is more ductile, so the elements resist higher deformations before the deletion criterion is triggered, resulting in fewer elements deleted and a more voluminous chip. It is known that chip morphology in FEM numerical simulations is highly dependent on the constitutive model used to describe the mechanical properties of the workpiece material, even for one single material. In their work, Thepsonthi and Özel [11] compared the use of viscoplastic and elasto-viscoplastic assumptions for describing the properties of Ti-6Al-4V in FEM simulations of micromilling. The authors observed that the chip changes from continuous to fragmented when elasto-viscoplastic assumption is used instead of viscoplastic. The authors claim that when the viscoplastic assumption is used, the elastic deformation is negligible in comparison with the plastic deformation, which can drastically simplify the problem and reduce computational time.

Figure 4 also shows that the maximum values of von Mises stress for Inconel 718 are considerably higher than Al 6101-T6. For example, in the third frame shown, the maximum von Mises stress for the nickel superalloy was 2,404 MPa, whereas this parameter reached only 774.5 MPa for the aluminum alloy, at the same machined length, which represents a difference of around 340%. High values of residual stress are directly associated with poor surface quality, which is a recurrent problem in machining of Inconel 718. Silva, da Silva and Oliveira [12] evaluated the surface quality of microslots of Inconel 718, manufactured with tungsten carbide tools with 400 µm of diameter. The authors observed that the surface roughness R_a was greater than 0.140 µm for all the slots, whereas Kumar, Deb and Paul [13] obtained R_a smaller than 0.090 µm in microslots obtained under similar conditions in Al 6101-T6. Therefore, the aluminum alloy is expected to present better surface quality.

3.2 Cutting forces

The forces acting on the workpiece were monitored in each time interval. A comparison of the cutting forces for both workpiece materials is shown in Fig. 5.

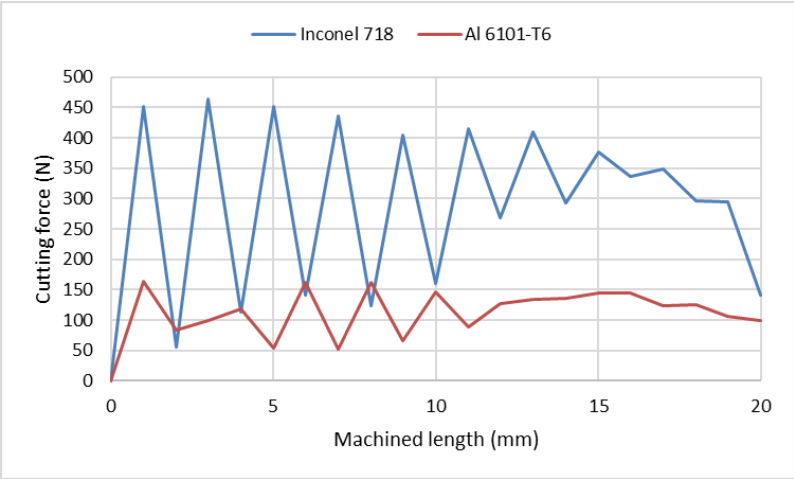

Figure 5. Chip morphology and von Mises stress distribution for Al 6101-T6.

From Fig. 5, it is possible to notice that there are significant irregularities in the maximum value of force throughout the machined length, with high amplitude between peaks of force, for both materials. This happens because the force is determined by the volume of material exerting pressure on the flank face of the tool, which is a parameter that varies irregularly according to the number of elements deleted by the failure criterium and the continuity of the chip. Furthermore, the values of maximum cutting force for the nickel superalloy (approximately 450 N) are roughly three times as big as the equivalent values for aluminum (approximately 150 N). This is expected, considering that the densities of the two materials are 8.19×10^{-6} kg/mm^3 and 2.70×10^{-6} kg/mm^3. Since the volume of the workpieces is the same, their masses differ by a factor of 3.03, and the forces differ accordingly when the other input parameters are maintained.

The high forces in machining of Inconel 718 are known as one of the reasons for its low machinability. Bartolomeis et al. [14] conducted an extensive review work on the machinability of this superalloy. According to the authors, the thermomechanical stresses induced by high cutting forces and cutting temperature gradients cause damage to the machined surface, as well as rapid tool wear and microstructure and mechanical properties alterations.

4 Conclusions

In this work, simulations of machining were conducted using Abaqus. Two models of workpiece were used to represent the mechanical properties of two different materials, namely Inconel 718 and Al 6101-T6. The following conclusions can be drawn:

- Chips of Al 6101-T6 tend to be thicker than Inconel 718 due to the higher ductility of aluminum.
- Machining of Inconel 718 result in residual stresses more than two times greater than Al 6101-T6, generating worse surface quality of the machined part.
- Cutting forces during machining of Inconel 718 can be up to three times greater than Al 6101-T6, which is associated with higher rates of tool wear.

Acknowledgements. The authors are thankful to CAPES, CNPQ and the University of Brasília.

Authorship statement. The authors hereby confirm that they are the sole liable persons responsible for the authorship of this work, and that all material that has been herein included as part of the present paper is either the property (and authorship) of the authors or has the permission of the owners to be included here.

References

[1] W. Jinsheng, S. Jiashun, G. Yadong, G. Abba, C. Guangqi, A micro milling model considering metal phases and minimum chip thickness, Key Eng Mater. 375–376 (2008) 505–509. https://doi.org/10.4028/WWW.SCIENTIFIC.NET/KEM.375-376.505.

[2] T. Thepsonthi, T. Özel, 3-D finite element process simulation of micro-end milling Ti-6Al-4V titanium alloy: Experimental validations on chip flow and tool wear, J Mater Process Technol. 221 (2015) 128–145. https://doi.org/10.1016/J.JMATPROTEC.2015.02.019.

[3] J.P. Davim, Machinability of Advanced Materials | Materials Characterization | General & Introductory Materials Science | Subjects | Wiley, (n.d.) 256. https://www.wiley.com/en-us/Machinability+of+Advanced+Materials-p-9781848213968 (accessed July 3, 2023).

[4] I.P. Okokpujie, L.K. Tartibu, A mini-review of the behaviour characteristic of machining processes of aluminium alloys, Mater Today Proc. 62 (2022) 4526–4532. https://doi.org/10.1016/J.MATPR.2022.05.006.

[5] G.R. Thellaputta, P.S. Chandra, C.S.P. Rao, Machinability of Nickel Based Superalloys: A Review, Mater Today Proc. 4 (2017) 3712–3721. https://doi.org/10.1016/J.MATPR.2017.02.266.

[6] P.K. Jain, P. Baredar, S.C. Soni, Microstructure and mechanical properties of silicon carbide particle reinforced aluminium 6101 metal matrix composite produced by two-step stir casting, Mater Today Proc. 26 (2020) 2740–2745. https://doi.org/10.1016/J.MATPR.2020.02.573.

[7] Y. Liu, D. Xu, M. Agmell, R.M. Saoubi, A. Ahadi, J.E. Stahl, J. Zhou, Numerical and experimental investigation of tool geometry effect on residual stresses in orthogonal machining of Inconel 718, Simul Model Pract Theory. 106 (2021) 102187. https://doi.org/10.1016/J.SIMPAT.2020.102187.

[8] G.R. Johnson, W.H. Cook, Fracture characteristics of three metals subjected to various strains, strain rates, temperatures and pressures, Eng Fract Mech. 21 (1985) 31–48. https://doi.org/10.1016/0013-7944(85)90052-9.

[9] B. Erice, F. Gálvez, A coupled elastoplastic-damage constitutive model with Lode angle dependent failure criterion, Int J Solids Struct. 51 (2014) 93–110. https://doi.org/10.1016/J.IJSOLSTR.2013.09.015.

[10] L. Malcher, L.L.D. Morales, V.A.M. Rodrigues, V.R.M. Silva, L.M. Araújo, G. V. Ferreira, R.S. Neves, Experimental program and numerical assessment for determination of stress triaxiality and J3 effects on AA6101-T4, Theoretical and Applied Fracture Mechanics. 106 (2020) 102476. https://doi.org/10.1016/J.TAFMEC.2020.102476.

[11] T. Thepsonthi, T. Özel, Simulation of serrated chip formation in micro-milling of titanium alloy Ti-6Al-4V using 2D elasto-viscoplastic finite element modeling, Production Engineering. 10 (2016) 575–586. https://doi.org/10.1007/S11740-016-0701-8.

[12] G. de Paiva Silva, M. Bacci da Silva, D. de Oliveira, Influence of abrasive deburring in indirect tool wear measurement in micromilling of Inconel 718, Journal of the Brazilian Society of Mechanical Sciences and Engineering. 45 (2023) 1–10. https://doi.org/10.1007/S40430-023-04190-1/FIGURES/11.

[13] A.S. Kumar, S. Deb, S. Paul, A study on micro-milling of aluminium 6061 and copper with respect to cutting forces, surface roughness and burr formation, ASME 2018 13th International Manufacturing Science and Engineering Conference, MSEC 2018. 4 (2018). https://doi.org/10.1115/MSEC2018-6570.

[14] A. De Bartolomeis, S.T. Newman, I.S. Jawahir, D. Biermann, A. Shokrani, Future research directions in the machining of Inconel 718, J Mater Process Technol. 297 (2021) 117260. https://doi.org/10.1016/J.JMATPROTEC.2021.117260.